

Diurnal Cycles of Cumulus, Cumulonimbus, Stratus, Stratocumulus, and Fog from Surface Observations over Land and Ocean

RYAN EASTMAN AND STEPHEN G. WARREN

Department of Atmospheric Sciences, University of Washington, Seattle, Washington

(Manuscript received 20 June 2013, in final form 9 December 2013)

ABSTRACT

A worldwide climatology of the diurnal cycles of low clouds is obtained from surface observations made eight or four times daily at 3- or 6-h intervals from weather stations and ships. Harmonic fits to the daily cycle are made for 5388 weather stations with long periods of record, and for gridded data on a $5^\circ \times 5^\circ$ or $10^\circ \times 10^\circ$ latitude–longitude grid over land and ocean areas separately.

For all cloud types, the diurnal cycle has larger amplitude over land than over ocean, on average by a factor of 2. Diurnal cycles of cloud amount appear to be proprietary to each low cloud type, showing the same cycle regardless of whether that type dominates the diurnal cycle of cloud cover. Stratiform cloud amounts tend to peak near sunrise, while cumuliform amounts peak in the afternoon; however, cumulonimbus amounts peak in the early morning over the ocean. Small latitudinal and seasonal variation is apparent in the phase and amplitude of the diurnal cycles of each type. Land areas show more seasonality compared to ocean areas with respect to which type dominates the diurnal cycle.

Multidecadal trends in low cloud cover are small and agree between day and night regardless of the local climate.

Diurnal cycles of base height are much larger over land than over the ocean. For most cloud types, the bases are highest in the midafternoon or early evening.

1. Introduction

Clouds have two competing effects on surface temperature. They emit longwave (infrared) radiation throughout the day and night, causing a warming at the surface relative to a cloudless sky. When the sun is high during the day their effect on albedo exceeds their reduction of longwave emission to space, causing cooling. Globally averaged, the negative shortwave cloud radiative effect (CRE; 47 W m^{-2}) exceeds the positive longwave CRE (26 W m^{-2}), so that clouds have a net cooling effect of 21 W m^{-2} (Loeb et al. 2009). The radiative effect of clouds is strongly negative during the daytime and strongly positive at night, so to assess the effects of cloud cover changes on climate it is important to determine the diurnal cycles of the clouds and to determine whether regional cloud amount changes are occurring during daytime or at night, or both. Even in a steady climate, when computing the net CRE it is important to take the

diurnal cycle into account to avoid biases. Rozendaal et al. (1995) showed that cloud radiative forcing is overestimated by 3 W m^{-2} both at the surface and at the top of the atmosphere if a diurnal average cloud amount is used rather than a diurnal cycle.

Low clouds respond to the day–night cycle of solar flux. During daytime clouds form due to the destabilization of the boundary layer by solar heating of the surface, driving convection and generating cumuliform clouds. At night the boundary layer cools, eventually causing condensation to form stratiform clouds. Stratiform cloud tops then cool as they emit longwave radiation to space, causing overturning within, sustaining the cloud deck. Maritime convection can also be enhanced at night by cloud-top cooling relative to nearby clear areas (Gray and Jacobson 1977). Daytime surface heating and nighttime radiative cooling are the two principal drivers of the diurnal cycles of low clouds.

Studies of the diurnal cycles of cloud cover have been carried out using a variety of satellite datasets (Wylie 2008; Stubenrauch et al. 2006; Kondragunta and Gruber 1996; Rozendaal et al. 1995; Bergman and Salby 1996, among others). Satellites look down at the earth from

Corresponding author address: Ryan Eastman, Atmospheric Sciences, Box 351640, University of Washington, Seattle, WA 98195.
E-mail: rmeast@atmos.washington.edu

above, so high clouds often obscure their view of low clouds, requiring assumptions about overlap to infer the coverage of low clouds. This paper will instead examine the diurnal cycles of clouds with low bases as seen from the surface, so no assumptions about overlap are needed. Surface observers are closer to the clouds than satellites are, so they are able to resolve individual clouds and identify clouds by type. The standard reporting code allows for nine types of low clouds, and an estimate of the base height is also reported.

Many of the previously mentioned climatologies focus either on a particular cloud type or a particular region. In this work we use a much broader approach, analyzing five cloud types over much of the surface of Earth using a single data source. In our climatology we use surface observations beginning in 1954 over the ocean and in 1971 over land. Cloud types and amounts are reported by trained observers at weather stations and by volunteer observers on ships spanning most of the globe. These observations have been processed, quality-controlled, and averaged into a climatology that we have made available to the user community. In this paper we will show how visual observations of clouds from below can quantify the diurnal cycles of low cloud types, and how those cycles vary with location around Earth.

2. Data

Cloud observations used in this study come from weather reports at fixed weather stations on land, or from ships. In the Arctic, observations are taken from manned research stations floating on sea ice. All surface observations used here were reported in the “synoptic” code of the World Meteorological Organization (WMO). Cloud cover is reported in octas (eighths) at three levels: low, middle, and high. At each level one of nine possible cloud types is specified, giving a total number of 27 possible types (WMO 1956, 1974).

Observations at land stations are typically taken 8 times a day at UTC hours divisible by 3 (0000, 0300, 0600 UTC, etc.), with some deviations (e.g., some Australian stations report at *local* times divisible by 3). Observations from ships are usually taken only 4 times a day, every 6 h, but about 15% of the ships do report at 3-h intervals. Ocean data are stored for individual 10° grid boxes with longitude bounds increasing poleward of 50° , keeping the box sizes roughly “equal area.” In some ocean grid boxes there was a tendency for cloud amounts averaged at 0300, 0900, 1500, and 2100 UTC to be consistently higher or lower than those averaged at 0000, 0600, 1200, and 1800 UTC. Although we were not able to determine which is “truth,” there were substantially more observations at 0000, 0600, 1200, and

1800 UTC compared with the other times, so over the ocean we used only those made at 0000, 0600, 1200, and 1800 UTC, except where noted otherwise.

Clouds at night are often not sufficiently illuminated to be reported accurately, so we screen the nighttime observations for adequacy of moonlight or twilight (Hahn et al. 1995). Our illuminance criterion permits the use of about 38% of the nighttime observations. Middle and high clouds are not included in this study since nighttime detection at those levels is more difficult, and there may be a residual underreporting even in observations that satisfy our criterion. Furthermore, the random-overlap assumption we use for middle and high clouds (Eastman et al. 2011; Eastman and Warren 2013) may not produce representative cloud amounts throughout the diurnal cycle given the already strong diurnal cycles of low cloud decks and the shortcomings of the random-overlap assumption when dealing with convection (Weare 1999).

Our source of synoptic observations from ships is the International Comprehensive Ocean–Atmosphere Data Set (ICOADS; Woodruff et al. 1987, 1998; Worley et al. 2005). For cloud reports from weather stations we used the archive of the Fleet Numerical Meteorology and Oceanography Center (FNMOC) from 1971 to 1976, then the National Centers for Environmental Prediction (NCEP) from 1977 to 1996. From 1997 to 2009 we found the best data source to be the Integrated Surface Database (ISD; Smith et al. 2011). The number of available observations per year has decreased during the past several decades. In 2008, ship observations were reported at a rate of around 400 000 per year, down from a peak in the 1980s of 1.5 million observations per year (Fig. 1 of Eastman et al. 2011). Over land, observations have also decreased from a peak of 7.5 million per year in the 1980s to 3.2 million per year in the 2000s. This decline is largely caused by most U.S., Canadian, and New Zealand weather stations dropping out of the worldwide reporting network as they instituted automated cloud-detection systems using laser ceilometers, phasing out visual surface observations. These changes in observation type create discontinuities in the data, so automated observations are not included in our dataset.

Observations were collected and processed into a single, uniform archive called the Extended Edited Cloud Reports Archive (EECRA; Hahn et al. 2009). Information about cloud type, level, amount, and low-cloud base height is accompanied by relevant meteorological information such as temperature, wind, sea level pressure, and dewpoint. This archive of surface observations is available through the Carbon Dioxide Information Analysis Center (CDIAC) as dataset NDP-026C (<http://cdiac.ornl.gov/epubs/ndp/ndp026c/ndp026c.html>).

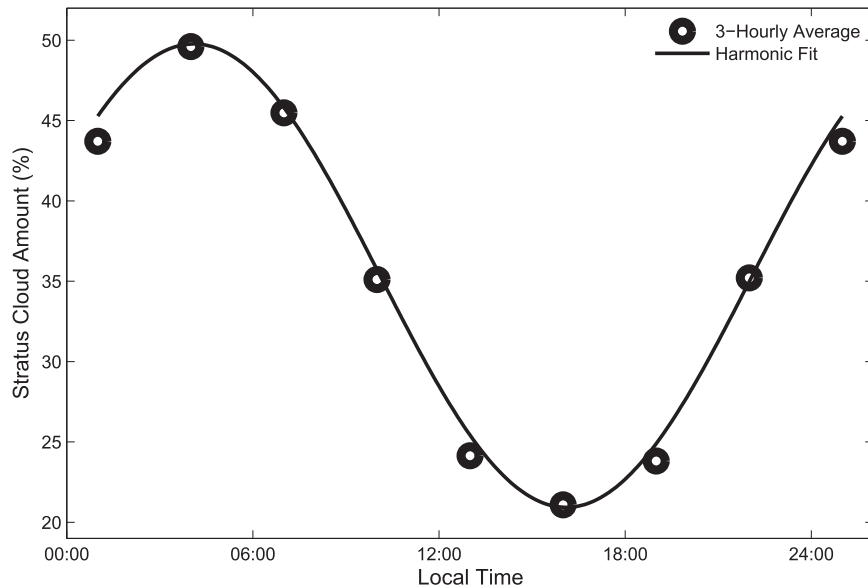


FIG. 1. Three-hourly average cloud amounts and their first harmonic fit for stratus clouds in March–May at station 57902, Xingren, China (25.5°N, 105.2°E). Data are available in both forms in this climatology.

Using the EECRA we created a climatology of averaged cloud amounts. The 27 cloud types of the synoptic code have been grouped into nine types for our analyses. The nine types include a single high (cirriform) type, three middle types (nimbostratus, altostratus, and alto-cumulus), and the five low types that are the focus of this study [fog, stratus (St), stratocumulus (Sc), cumulus (Cu), and cumulonimbus (Cb)]. Cumulonimbus is a vertically developed cloud whose top may be at the high-cloud level, but because its base is within 2 km of the surface it is reported as a “low” cloud in the synoptic code. Average amounts of a given cloud type are calculated by multiplying its amount (when present) by its frequency of occurrence over a specified period of time (month or season). As an example, if cumulus was present in 30% of the observations in one month, and the average Cu sky cover was 25%, then the average amount of Cu for that month would be 0.3×0.25 , or 7.5%. More details about processing procedures are given by Hahn et al. (2003, 2007, 2009).

Files containing average cloud amounts and frequencies are available in our climatology. Averages are available for 10° grid boxes over the ocean and 5° boxes over land (Hahn et al. 2007). Longitude bounds are expanded near the poles to keep the area represented by each box roughly equal. Averages are also available for each of 5388 selected weather stations (Hahn et al. 2003). Long-term averages use data from 1954 to 1997 over the ocean and from 1971 to 1996 over land areas. These long-term-average files contain average cloud amounts and

frequency of occurrence for seasons or months. Averages for individual years are also available in this climatology on the seasonal and (for land only) monthly time scales. These yearly averages have been updated through 2008 over the ocean and 2009 over land.

Long-term averages and frequencies of occurrence are available for day and night separately as well as for each 3-h interval throughout the 24-h period. There are insufficient numbers of observations to produce reliable 3-hourly averages for individual years, so we do not investigate the interannual variation of diurnal-cycle amplitude and phase. Files in the database also list the number of observations that have gone into each 3-hourly average cloud amount or base height. In this study we require at least 50 observations per 3-h time period. As mentioned above, data over the ocean showed some inconsistencies at 3-h intervals. Although data files contain averages for every 3-h period, for ocean data in this work we only use averages at a 6-h interval, taken at 0000, 0600, 1200, and 1800 UTC. An exception is made only for the computation of the first harmonic discussed below, where (for roughly 39% of available grid boxes) all available points were used to construct a cosine curve fit to the diurnal cycle.

The first harmonic function (cosine curve) was fit to the 24-h plots of these 3- or 6-hourly averages as is shown in Fig. 1. These functions represent a single wave with a period of 24 h fit to the data, and are available in separate files. The files contain all the necessary information to recreate the wave, including the phase

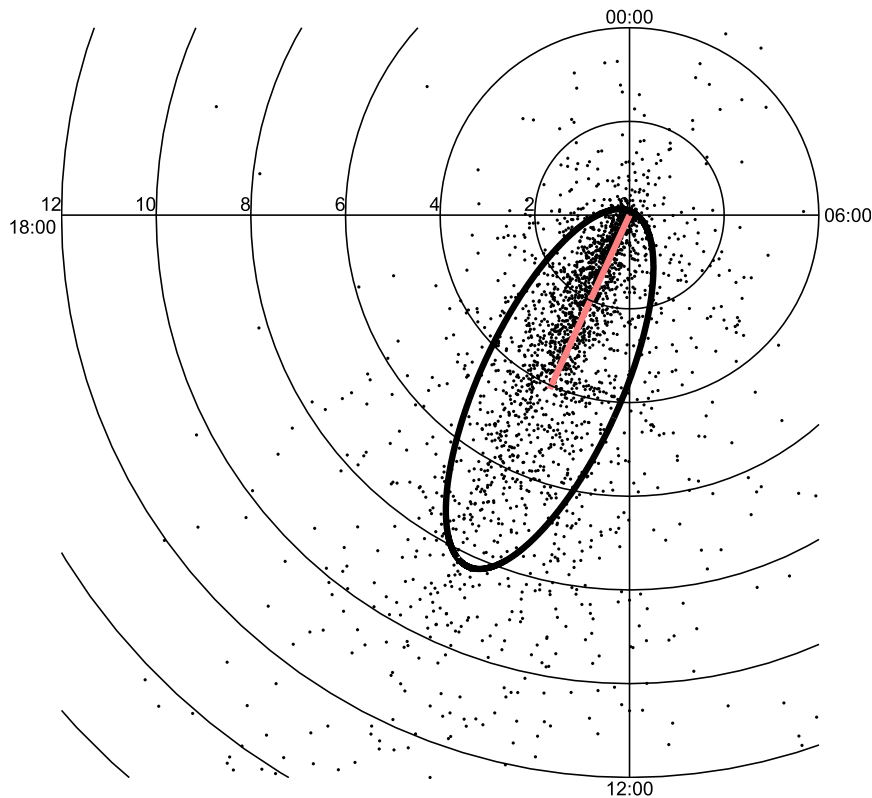


FIG. 2. An example ellipse showing the distribution of endpoints of individual phase/amplitude vectors (dots), the area-weighted mean vector (pink line), and the ellipse centered on the mean vector. The major and minor ellipse axes are determined by the area-weighted standard deviation parallel and perpendicular to the mean vector's direction. Local time is shown on the axes; magnitude is represented by the distance from the origin. This example uses data from cumulus clouds over land in all seasons (the pink ellipse in Fig. 3a).

(time of local maximum) and amplitude (half of the distance from peak to valley) of the cosine curve. The variance explained by the harmonic fit is also given, since many fits are not as ideal as that shown in Fig. 1. If a grid box has too few samples at a given time, the cloud amount at that time does not contribute to the fit. This is especially relevant over the remote ocean where about 61% of the grid boxes have suitable data only at 6-h intervals, so the cosine curve is fit to only four points. Further details about these fits are available in Hahn et al. (2007). In this paper we give some examples of how surface observations can be used to investigate climatic characteristics of the diurnal cycles of low clouds.

3. Results

a. Global perspective

Figures 2 and 3 show ellipses fit to scatterplots of phase and amplitude vectors for individual grid boxes. Vector magnitude is represented as the distance from

the origin; phase (time of local cloud maximum) is shown by the vector direction on the 24-h clock. These figures were made using the harmonic fits described above. Figure 2 is an illustration of how ellipse dimensions were calculated, with dots representing the end points of vectors for each individual grid box, and the mean vector (land/ocean area weighted) plotted as a thick line. The ellipse is centered on the vector mean. The extents of the major and minor ellipse axes are based on the area-weighted standard deviations in vector space. Ranges of amplitude and phase for each cloud type are shown in Fig. 3. Land and ocean are shown separately.

Figure 3 shows that the diurnal cycles have larger amplitude over land than over ocean for every cloud type. This is an expected result since the land surface has a lower thermal inertia than the ocean, so the land surface temperature undergoes a larger diurnal cycle. Cumuliform clouds have the largest average cycle over land, while stratiform, particularly Sc, dominates the diurnal cycle over the oceans. Most cloud types exhibit

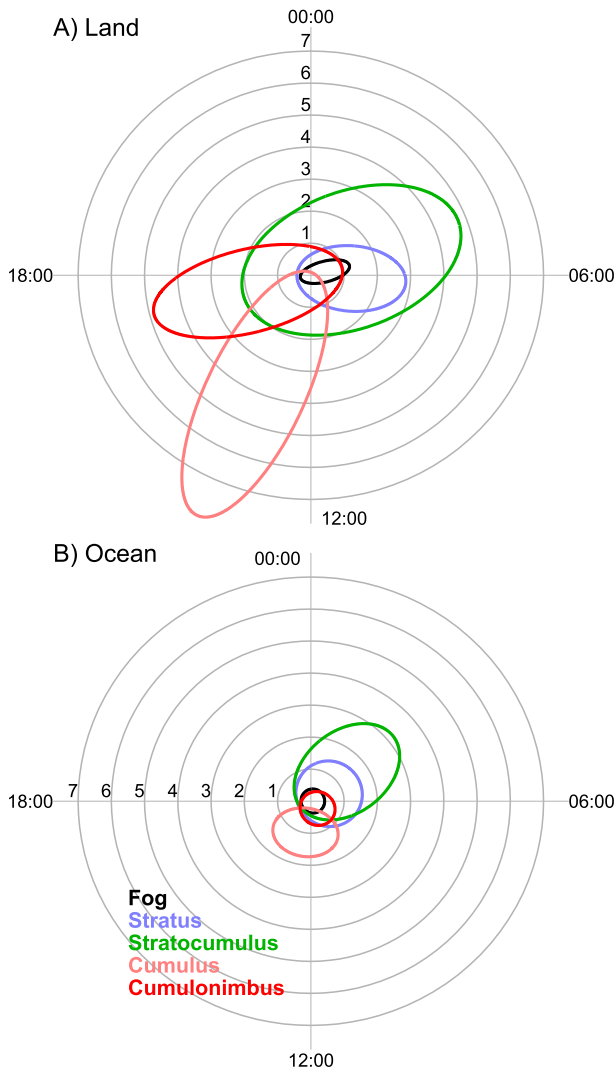


FIG. 3. Ranges of amplitude and phase for each cloud type for (a) land areas and (b) ocean areas. Each ellipse is centered on the endpoint of the mean diurnal phase/amplitude vector. All seasons are included. The mean vector is the area-weighted vector average of phase/amplitude vectors for each grid box. The major and minor ellipse dimensions represent the area-weighted standard deviations in and perpendicular to the vector direction. Times are local time; vector magnitude is the distance from the origin.

similar phase over both ocean and land with the exception of Cb, which peaks in the afternoon over land but in the early morning over the ocean. This is due to differing mechanisms that drive convection—afternoon surface heating over land, but nighttime radiative cooling at cloud top over the ocean (Gray and Jacobson 1977). Stratiform cloud amounts tend to peak in the morning while (with the exception of oceanic Cb) cumuliform clouds peak in the afternoon. Stratus and Sc reach their maximum slightly later in the morning over land than over ocean.

Phases and amplitudes of low cloud types vary as a function of latitude. The latitudinal variations for the ocean are shown in Fig. 4. Phases are not shown for diurnal cycle amplitudes less than 0.25%. Fog shows an appreciable diurnal cycle only where fog is common, namely at high latitudes where fog shows a maximum at or slightly after midnight during summer, and a smaller maximum just after noon during winter. The maximum development of stratiform clouds (both St and Sc) occurs early in the morning in the tropics. During winter stratiform clouds tend to peak later in the day at higher latitudes, as do stratocumulus clouds during the arctic summer. Stratiform clouds show their largest diurnal cycles away from the equator, with stratocumulus clouds showing the strongest cycle in the extratropics and stratus clouds showing their strongest cycle poleward of the stratocumulus maxima. Stratiform clouds show stronger diurnal cycles during summer, except in Arctic winter. The diurnal cycle of cumulus clouds peaks around noon in the tropics and during midlatitude summer. The cumulus cycle peaks earlier in midlatitude winter. The magnitude of the cumulus diurnal cycle is stronger near the equator and in middle latitudes during summer. Cumulonimbus amounts are at their maximum near sunrise at the equator, but peak later in the day near the poles during winter and earlier near the poles during summer. Magnitudes of the cumulonimbus diurnal cycle are smallest of all cloud types over the ocean. The strongest diurnal cycles of cumulonimbus are seen over northern high latitudes during winter, where most of the oceanic cumulonimbus is the result of cold continental air advecting over warmer water, leading to snow showers reported as Cb.

Figure 5 shows the latitudinal variation of diurnal phases and amplitudes over land areas (including islands). Note that the amplitude scales in Figs. 4 and 5 are different, to accommodate the larger amplitudes over land. Fog peaks consistently in the morning around sunrise. Stratus and Sc both peak during the morning, with an earlier peak in summer, possibly due to the earlier sunrise; daytime heating may weaken both the circulations aloft and stability below cloud level that sustain the cloud decks (Hignett 1991; Duynkerke 1993; Wood 2012). Amplitudes of the St and Sc cycles appear largest near the equator and in the summer hemisphere. Amplitudes of cumuliform clouds show a latitudinal pattern similar to stratiform, but enhanced. Cumulus clouds show a very uniform phase, with a peak just after noon and almost no latitudinal or seasonal variation. Cumulonimbus clouds peak after cumulus and show an earlier peak during winter.

Figure 6 uses dot plots to show the geographic distribution of phases and amplitudes of stratocumulus over ocean and cumulus over land, the two cloud types with

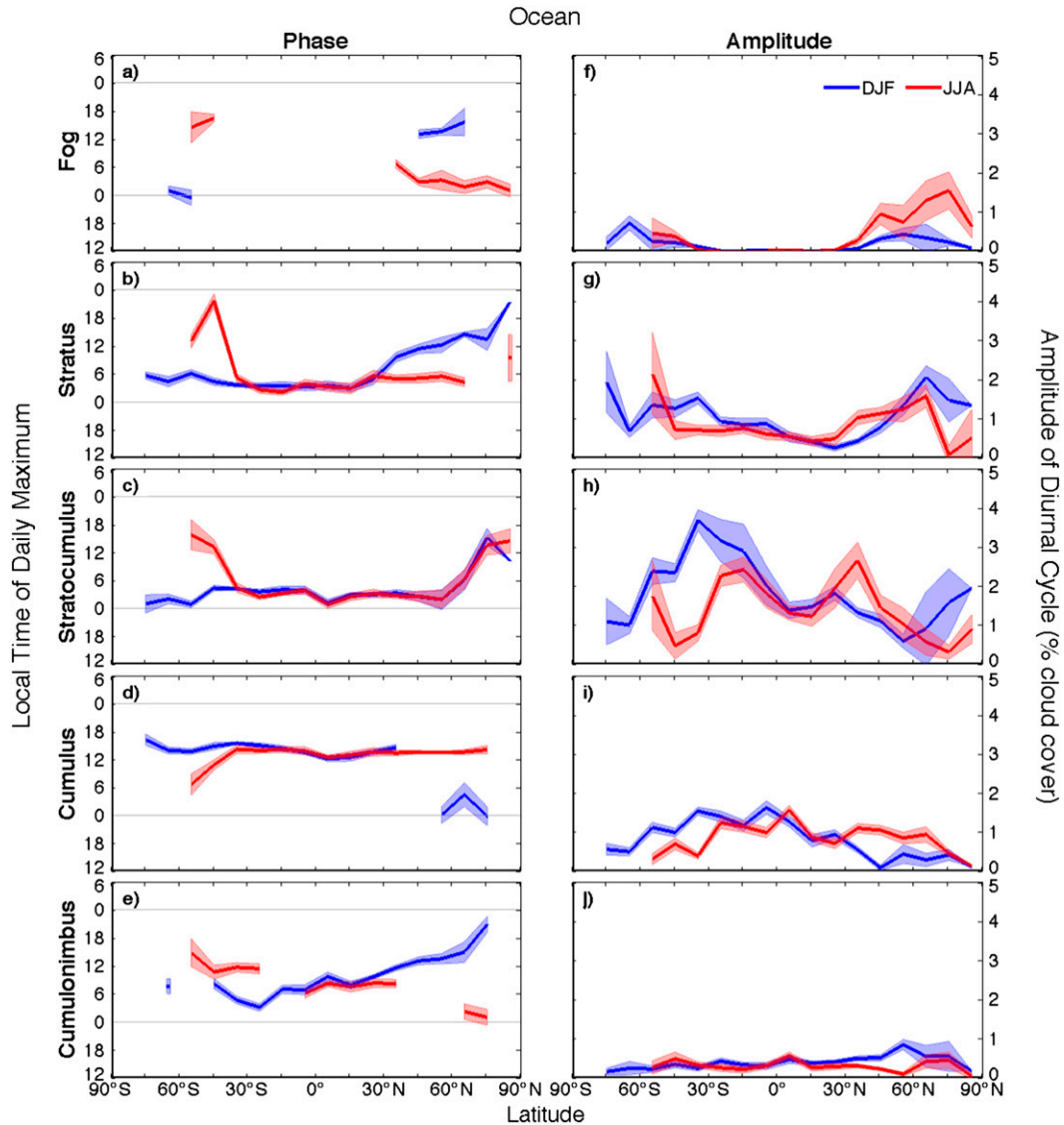


FIG. 4. The 10° zonal mean (a)–(e) phase and (f)–(j) amplitude of the diurnal cycles of the five cloud types over the ocean. Plots represent December–February (DJF; solid line) and June–August (JJA; dashed line). Zonal means are ocean-area-weighted vector averages from all available grid boxes within the zone. Phases are not plotted for diurnal amplitudes <0.25%. Error bars are the area-weighted standard error of the mean for each zone.

the most prominent diurnal cycles. Both maps are for June–August (JJA) only. Maps for the other low cloud types are not shown, but are available online (at www.atmos.washington.edu/CloudMap). Dot sizes indicate the magnitude of the diurnal cycle. Dot color represents the phase. These figures and their counterparts online show many strong geographical patterns, which users may apply to tasks requiring knowledge of the diurnal cycle. In Fig. 6, stratocumulus shows a morning peak, with higher-amplitude diurnal cycles in eastern ocean basins. Cumulus clouds show an afternoon peak, with higher-amplitude cycles in the summer hemisphere.

Analysis of the maps described above suggests that specific cloud types tend to dominate the diurnal cycle of low cloud in different geographic regions. Figures 7 and 8 show, for each grid box, which cloud type’s diurnal cycle has the largest magnitude. The cloud type with the largest cycle (which we call the “dominant” type) is represented by dot color; the amplitude of that cycle is represented by dot size. Amplitude data come from cosine curves fit to the 3- or 6-hourly averages.

These maps show that boxes with similar dominant types are clustered into coherent geographic regions. Stratiform types dominate the diurnal cycle over much

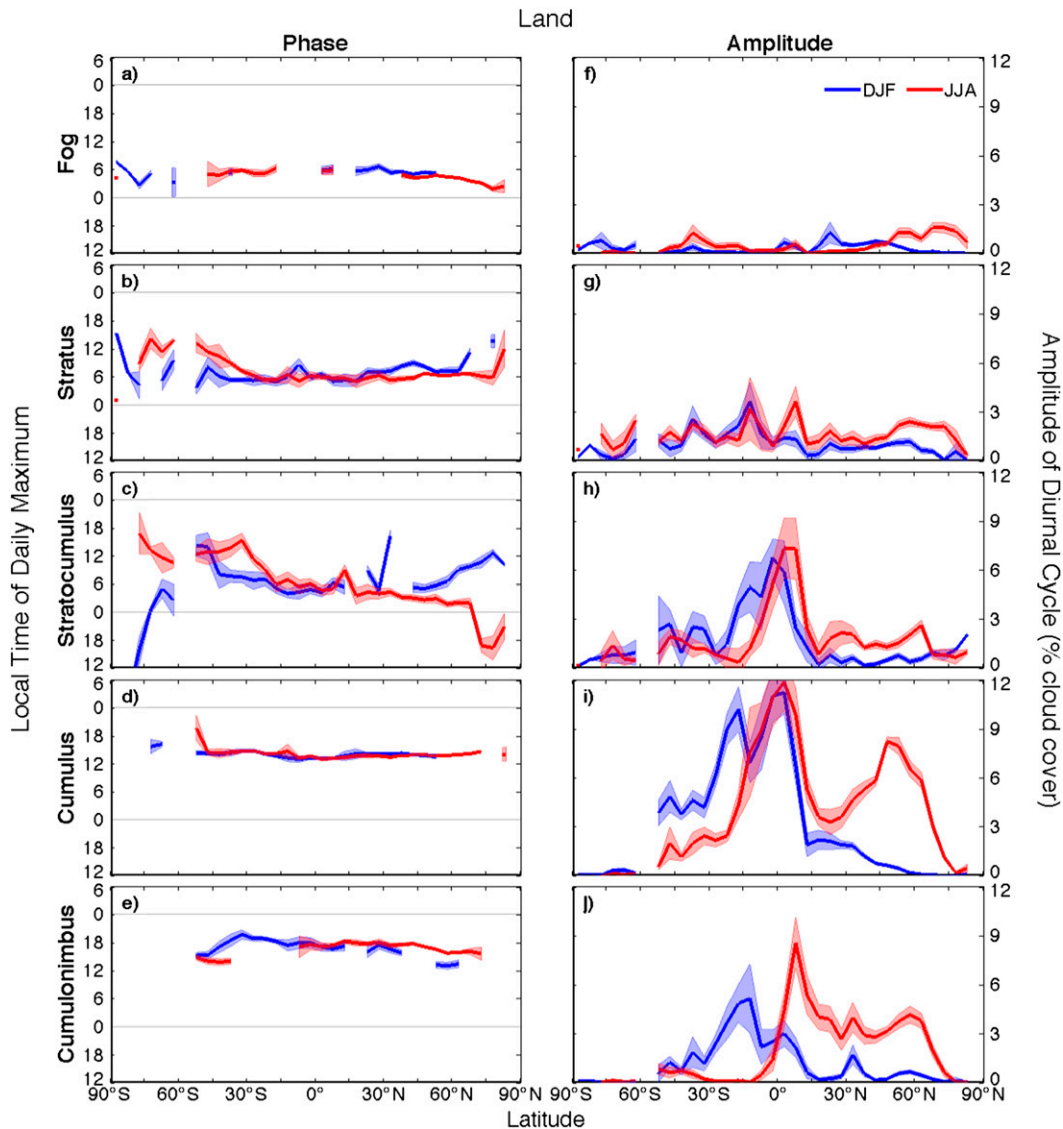


FIG. 5. As in Fig. 4, but for 5° zonal mean (a)–(e) phase and (f)–(j) amplitude.

of the ocean (Fig. 7) except near the equator, near land (particularly east coasts of continents), and at high latitudes during winter (where there is very little cycle). Seasonality is not particularly apparent over the ocean, with cycles in many regions dominated by either stratiform or cumuliform clouds throughout the year. However, fog is strongly seasonal; it dominates the diurnal cycle northeast of the northern continents only during summer. Much stronger seasonal shifts are seen over land (Fig. 8), especially in the Northern Hemisphere. Diurnal cycles over North America and Europe are small or dominated by St and Sc in winter, but by Cb and especially Cu during summer. The Himalayas and Rocky Mountains appear red in summer as Cb dominates their diurnal cycles. Siberia's diurnal cycle is also dominated by Cb throughout the year,

likely due to its distance downwind from the Atlantic Ocean. Stratiform clouds tend to dominate the diurnal cycle along the west coasts of all major continents throughout the year. Fog is dominant in a few regions that are very foggy in summer: Newfoundland, the Kuril Islands, and the coast of the Arctic Ocean.

b. Diurnal cycles of all cloud types as a function of dominant cloud type

The maps from Figs. 7 and 8 are used to segregate cloud data based on the cloud type that dominates the diurnal cycle in each grid box. Data were divided into five subsets, one for each dominant type. Each subset contains only those boxes that have the same dominant type (and for each box only those seasons in which the

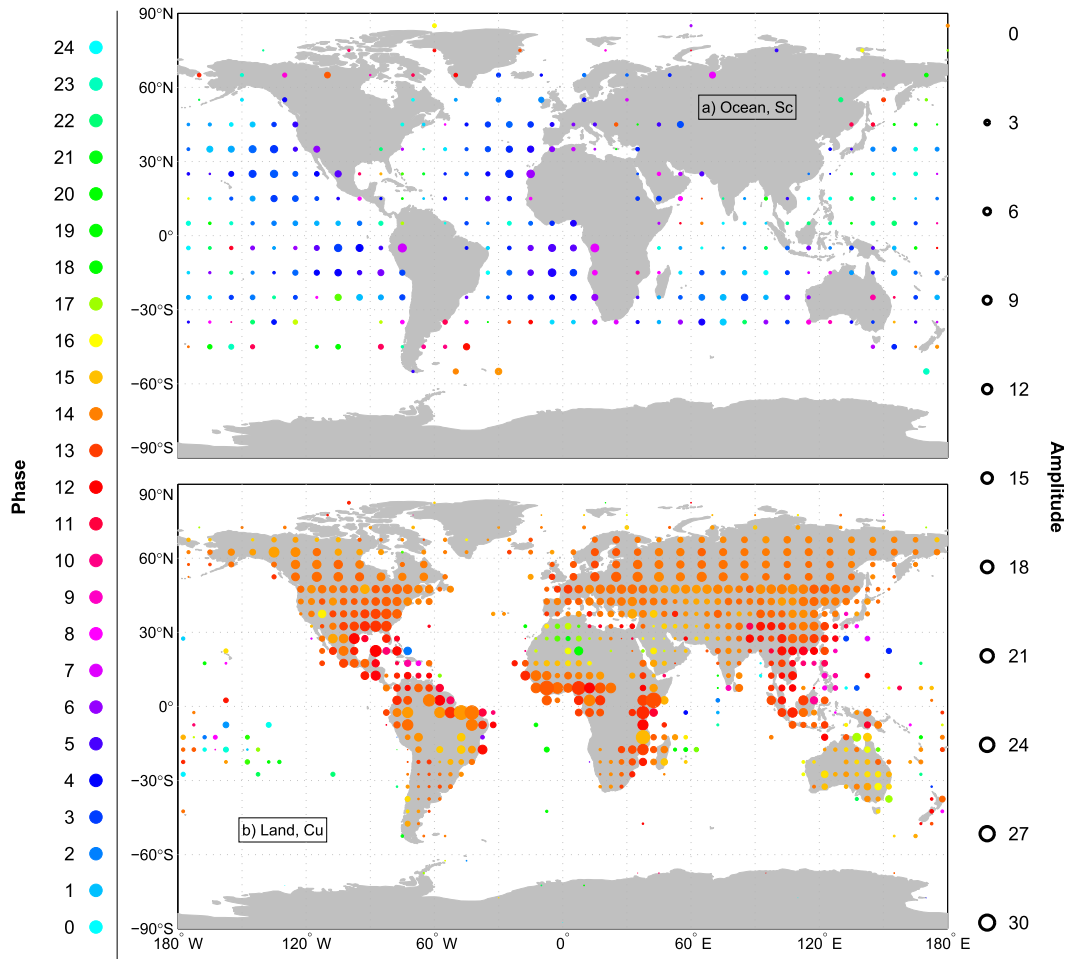


FIG. 6. Phase (color) and amplitude (proportional to dot area) of the diurnal cycle of (a) stratocumulus clouds over the ocean and (b) cumulus clouds over land, both during JJA. Dots are shown at the centers of all available $5^{\circ} \times 5^{\circ}$ (land) and $10^{\circ} \times 10^{\circ}$ (ocean) latitude-longitude equal-area grid boxes.

type is dominant); we call this subset a “regime.” A subset contains gridbox data for all low types, not just the dominant type. Figures 9 and 10 are made using area-weighted averages of 3-hourly (over land) or 6-hourly (over ocean) cloud amounts from each subset. Each data point represents the average cloud amount that occurred within the 3-h period (local time) surrounding the point in each contributing box over land, and 6-h period over the ocean. Some regimes over the ocean contain only a few boxes.

This analysis seeks to differentiate cloud behavior between and within differing regimes. Specifically, we hope to see how diurnal cycles of different clouds behave relative to one another in each regime and also to see whether the cycle of the same cloud type tends to have the same phase in differing regimes.

Figure 9 shows the diurnal cycle of each cloud type in each regime. Cloud type is represented by the color of

the line, using the same color key as in Figs. 7 and 8. The cloud type with the highest-amplitude diurnal cycle is not always the most common type. Over the ocean Sc is most prevalent in all regimes except Cu, even though it is not the dominant driver of the diurnal cycle in fog, St, and Cb regimes. In oceanic Cu regimes, Cu is the most common type, with Sc a close second. Over land Sc is also most prevalent in all regimes, although Cu and Cb show afternoon peaks higher than the Sc maximum. Each cloud type tends to have the same phase regardless of the regime it is in. This tendency is further explored in Fig. 10.

Figure 10 uses the same data from Fig. 9, but normalizes each cycle between 0 and 1 to facilitate comparison. Instead of each frame showing different types in each regime, frames in Fig. 10 show the diurnal cycle of the same type in differing regimes, with line color representing the regime rather than the type whose diurnal cycle is plotted. Cycles are omitted if their amplitudes

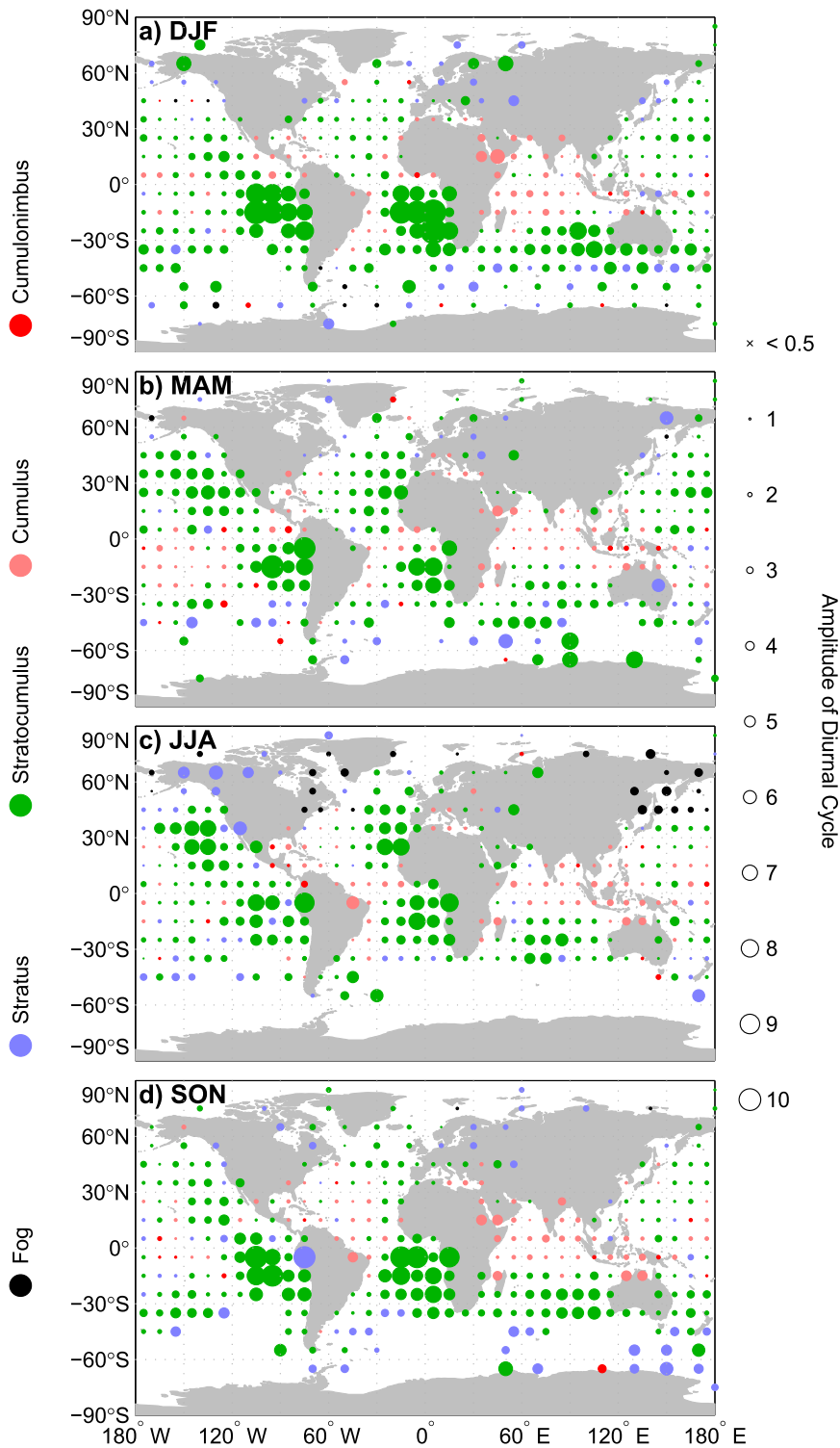


FIG. 7. Dots indicating the low cloud type whose diurnal cycle has the largest amplitude within that grid box. Dot color represents the type while dot size represents the amplitude of the cycle. Regions with diurnal cycles of magnitudes less than 0.5% are indicated by diagonal crosses; grid boxes with insufficient data are left blank. Ocean areas only.

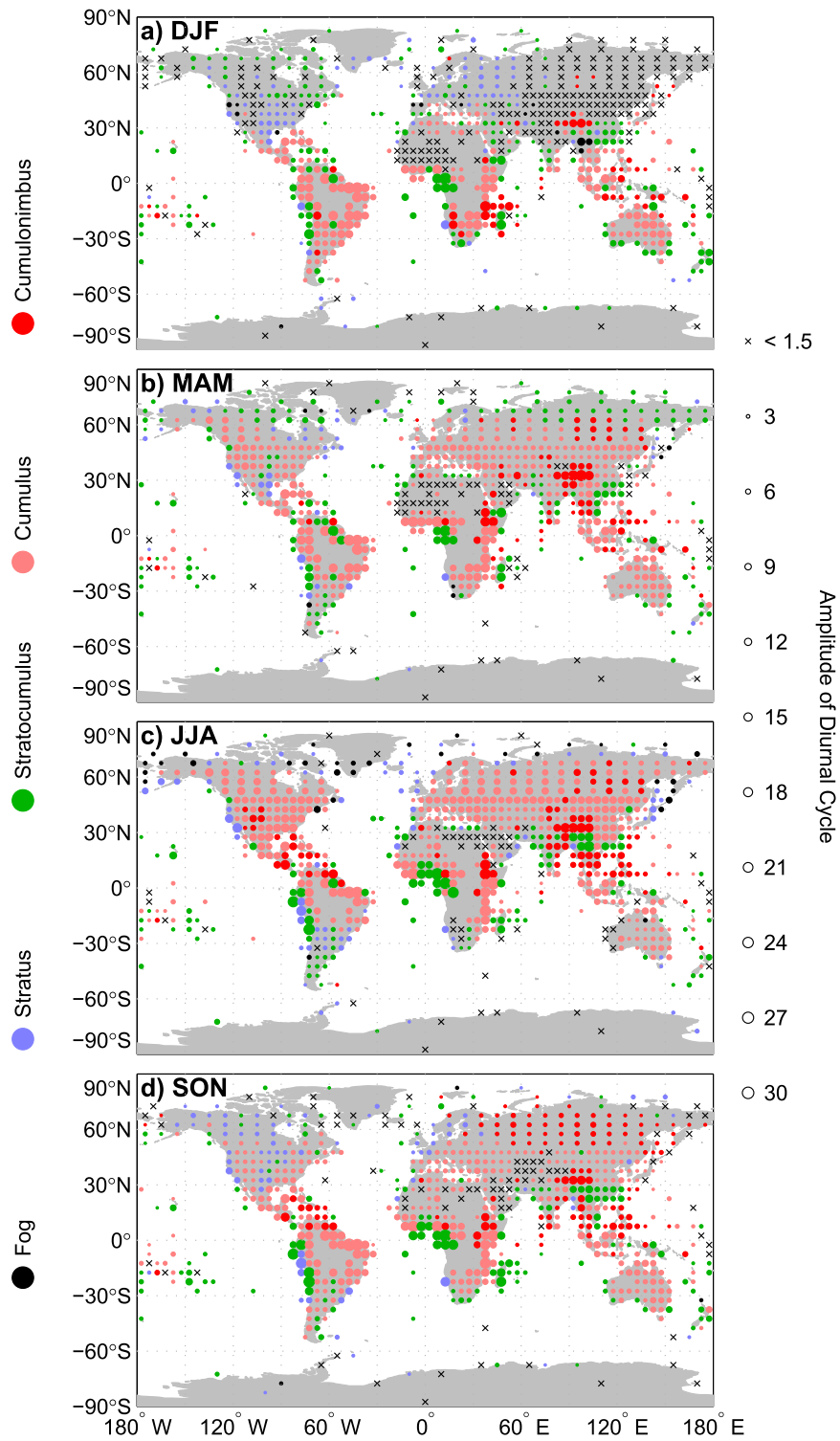


FIG. 8. As in Fig. 7, but for land. Regions with diurnal cycles of magnitudes less than 1.5% are indicated by diagonal crosses.

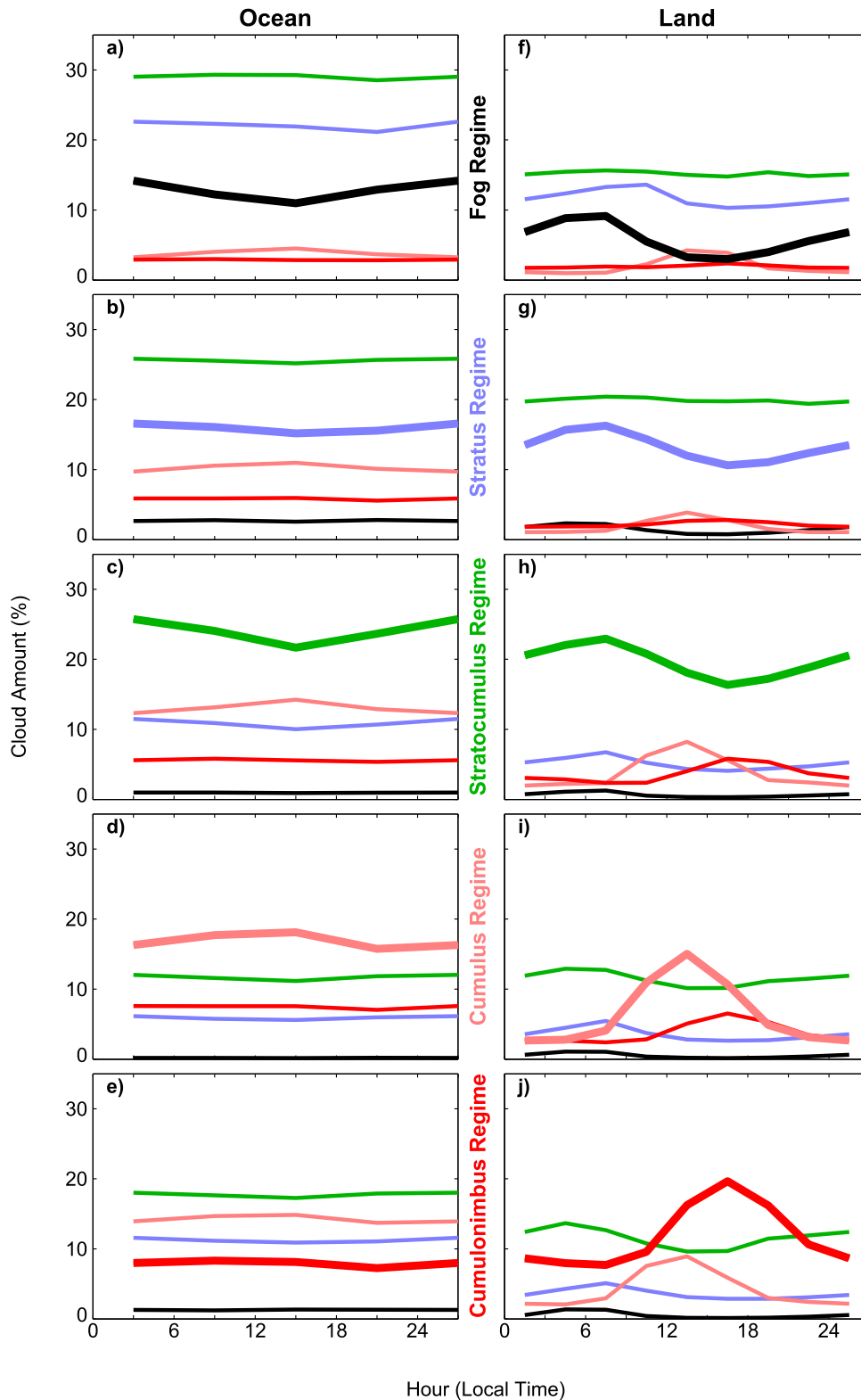


FIG. 9. Composed diurnal cycles of cloud types over (a)–(e) ocean (6-hourly averages) and (f)–(j) over land (3-hourly averages) in “regimes” defined as all grid boxes where the listed type shows the largest magnitude diurnal cycle. Line color corresponds to cloud type; type–color associations are shown as the color of the text describing each regime.

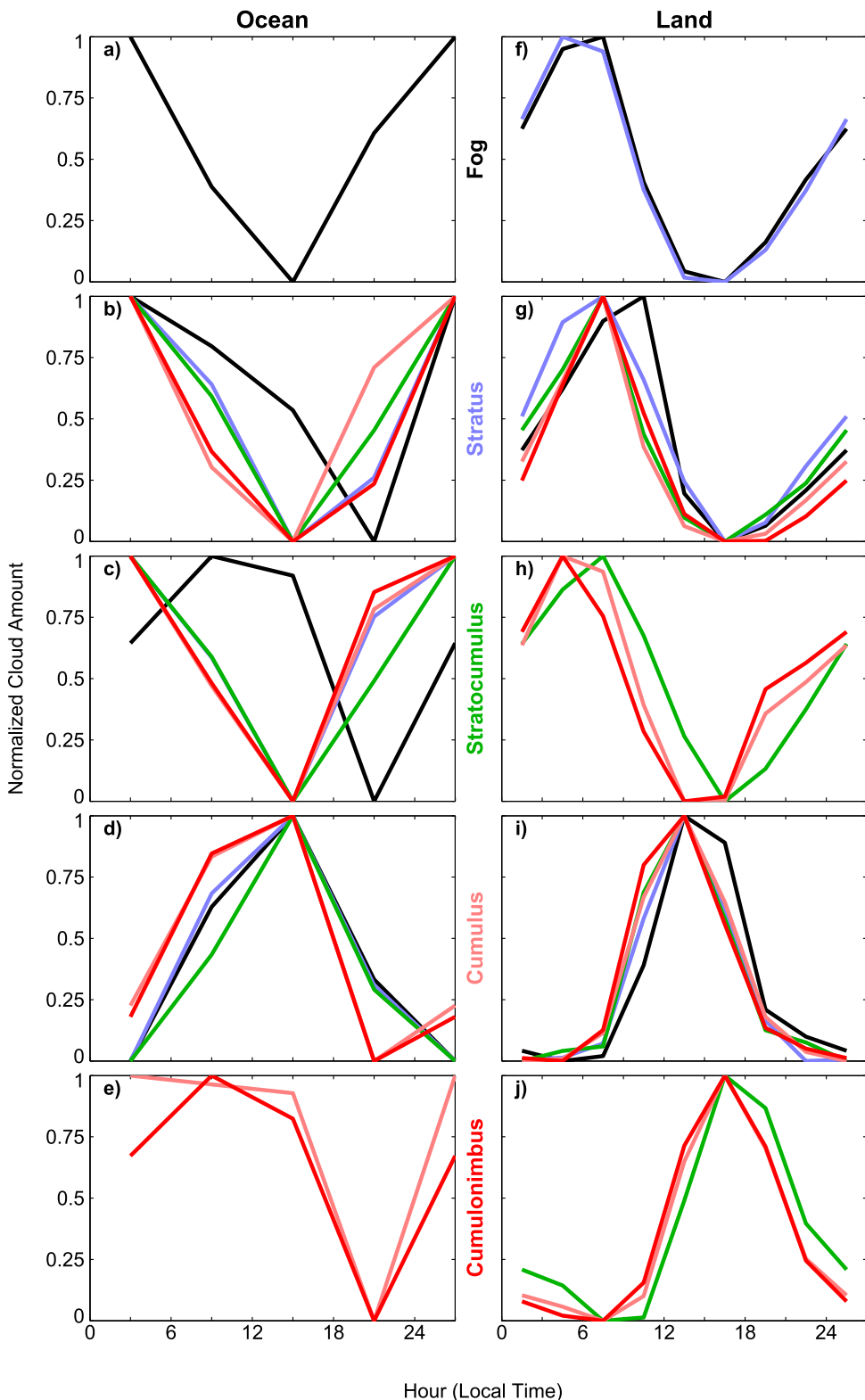


FIG. 10. Normalized diurnal cycles of cloud types over (a)–(e) ocean (6-h averages) and (f)–(j) land (3-h averages). Each frame [(a)–(j)] shows the diurnal cycle of the indicated type in each different regime. Line color indicates which regime is represented, corresponding to the color of the labels between the land and ocean columns. Normalized cycles are shown only if the diurnal cycle represented had a magnitude greater than 0.5% over the ocean or 1.5% over land.

are less than 0.5% over the ocean and 1.5% over land. The overlap of most of the lines in each frame supports the conclusion that each cloud type has a “proprietary” diurnal cycle, which is not heavily impacted by the climate regime. Cycles in fog regimes and for fog amounts are frequently omitted due to the small amplitudes of those cycles. Stratus and Sc do show a later peak in fog regimes, which is discussed further below.

c. Day versus night trends in amounts of low cloud types

Long-term, linear trends in cloud cover have been computed for day and night cloud amounts. Figure 3 of Warren et al. (2007) showed that nighttime trends in cloud cover over land tend to agree with daytime trends in both sign and magnitude. In Fig. 11 we show this to be the case by plotting day and night trends on the x and y axes respectively for both land and ocean areas in all seasons. We use average cloud amounts for individual years in each season to calculate trends, with time spans 1971–2009 over land and 1954–2008 over the ocean. All seasons are plotted together. Day and night average cloud amount files are also part of our cloud climatology and are available on our website. Trends are fit to time series using robust multilinear regression (iteratively weighted least squares with a bisquare weighting function) and are plotted in the figure only if they are 95% significant during both day and night. At least 20 years of data must be present in order to calculate a trend, with at least 20 observations per season. Also shown is the best-fit line to the scatterplot (red dashed). The 1:1 line is shown as a diagonal gray line.

Correlation between day and night trends is positive and significant for all cloud types in all seasons over both land and ocean. Slopes of the best-fit lines are shown. Some types show a consistently higher magnitude trend during one-half of the day. Over land cumulus clouds show a tendency for daytime trends to exceed nighttime trends, as do Cb. Fog and Sc over land show greater trends at night while St shows essentially no difference. Cumulus and Sc over the ocean show no difference between day and night trend magnitude, but fog, St, and Cb show greater trends at night, when those types are more prevalent. Generally, cloud types appear to either show no preference, or a greater trend during the half of the day when their amounts are greater. A detailed analysis of trends in all cloud types is available in Eastman et al. (2011) and Eastman and Warren (2013).

In Table 1 we use the regimes discussed previously to study trends in day and night cloud cover within each regime. Our goal is to investigate whether there are

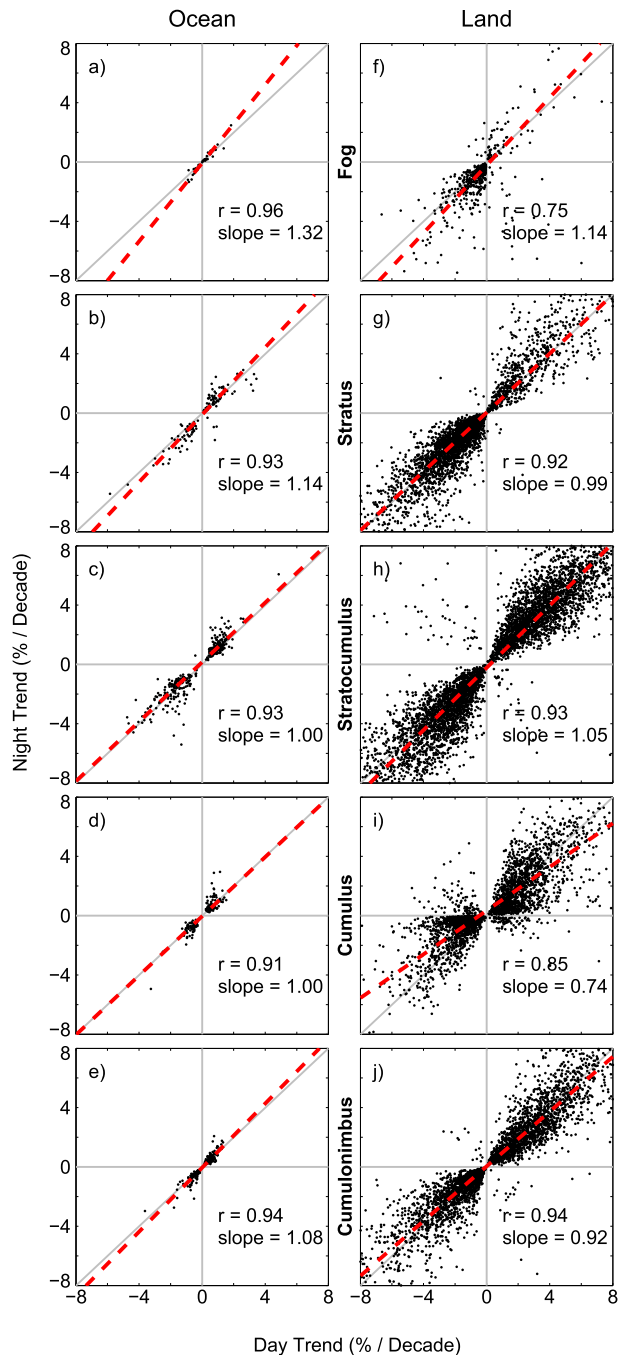


FIG. 11. Daytime vs nighttime trends with best-fit line (red dashed) for each low-cloud type. Each dot represents a grid box (ocean) or weather station (land) during one season. Trends and the best-fit lines are calculated using robust multilinear regression. The correlation coefficient (r) is given in each frame. Trends shown are for all four seasons, spanning 1971–2009 over land areas and 1954–2008 over the ocean. We require 20 observations per season per year, and both day and night time series must span a minimum of 20 years in order for a trend to be calculated. Trends are shown only if they are 95% significant during both day and night.

TABLE 1. Trends in cloud cover for each cloud type in each regime (regimes shown by dot color in Figs. 7 and 8) as well as for all regimes. Trends are calculated using robust multilinear regression and are given in percent per decade. For a grid box to contribute we require a minimum of 20 years with at least 20 observations per year. Trends are shown in bold if they are significant at the 95% level.

Ocean						
Day, trend (% decade ⁻¹)						
Type ↓ regime →	Fog	Stratus	Stratocumulus	Cumulus	Cumulonimbus	All regimes
Fog	-0.2	0	0	0	0	0
Stratus	-0.8	-0.1	0.1	0.1	-0.1	0.1
Stratocumulus	-0.6	-0.3	-0.3	0.7	0.3	0
Cumulus	0.4	0.1	0	-0.1	0.1	0
Cumulonimbus	0.2	0	0.1	-0.1	-0.1	0
Night, trend						
Type ↓ regime →	Fog	Stratus	Stratocumulus	Cumulus	Cumulonimbus	All regimes
Fog	-0.1	-0.1	0	0	0	0
Stratus	-0.9	-0.2	0	0	-0.2	0
Stratocumulus	-0.5	-0.4	-0.3	0.7	0.4	0
Cumulus	0.3	0.1	0	0	0.1	0
Cumulonimbus	0.1	0	0.1	-0.2	-0.1	0
Day – night, trend						
Type ↓ regime →	Fog	Stratus	Stratocumulus	Cumulus	Cumulonimbus	All regimes
Fog	-0.2	0.1	0	0	0	0
Stratus	-0.1	0.2	0	0.1	0.2	0.1
Stratocumulus	-0.1	0.1	0	0	-0.1	0
Cumulus	0.1	-0.1	0	-0.1	-0.1	0
Cumulonimbus	0	-0.1	0	0	0	0
Land						
Day, trend (% decade ⁻¹)						
Type ↓ regime →	Fog	Stratus	Stratocumulus	Cumulus	Cumulonimbus	All regimes
Fog	-0.3	-0.1	0	0	0	0
Stratus	-0.2	-0.4	-0.3	-0.4	-0.4	-0.4
Stratocumulus	0.8	0.8	0.5	0	0.3	0.2
Cumulus	0	0	-0.1	0	0	0
Cumulonimbus	0	0.1	0.1	0.1	0.2	0.1
Night, trend						
Type ↓ regime →	Fog	Stratus	Stratocumulus	Cumulus	Cumulonimbus	All regimes
Fog	-0.2	-0.2	-0.1	-0.1	-0.1	-0.1
Stratus	-0.1	-0.4	-0.2	-0.3	-0.4	-0.3
Stratocumulus	0.7	0.6	0.4	-0.1	0.4	0.2
Cumulus	0.1	0.1	0	0.1	0.1	0.1
Cumulonimbus	0	0.1	0.1	0.1	0.2	0.1
Day – night, trend						
Type ↓ regime →	Fog	Stratus	Stratocumulus	Cumulus	Cumulonimbus	All regimes
Fog	-0.1	0	0	0	0	0
Stratus	0	0.1	0	-0.1	-0.1	0
Stratocumulus	0.1	0.2	0.1	0.1	0	0
Cumulus	0	0	-0.1	-0.2	-0.1	-0.1
Cumulonimbus	0	0	-0.1	0	-0.1	-0.1

consistent changes taking place in geographically separate regions with similar climatologies. In each regime, time series are calculated from area-weighted yearly averaged anomalies from all contributing grid boxes. A trend line is fit to each time series. Day-minus-night cloud amount is calculated by subtracting the nighttime

time series from the daytime time series, and a trend line is fit to this day-minus-night time series. Time series over the ocean were analyzed after the global time series was subtracted from each gridbox time series, to remove as-yet-unexplained large-scale variations that appear to be spurious (Bajuk and Leovy 1998; Norris 1999; Eastman

et al. 2011). Numbers in Table 1 represent the trend in cloud amount for the cloud type (specified on the left) in each regime (specified across the top). Trends are shown in bold if they are 95% significant. A trend for all regimes, composed of all contributing grid boxes, is also shown.

In each regime the trends are generally less than 1% decade⁻¹. For ocean areas in stratiform regimes, Table 1 shows cumuliform clouds increasing at the expense of stratiform (first three columns of the table). The opposite is seen in cumuliform regions (columns 4 and 5). Stratocumulus shows the largest trends, increasing in cumuliform regimes while decreasing in stratiform regimes.

Over land fog is declining in fog and St regions, and St is declining in all regimes. Stratocumulus clouds are increasing in all regimes but Cu. Cumuliform clouds are showing low-magnitude, generally positive trends. Day-minus-night trends are small. Stratus clouds appear to be declining less at night while Cu clouds are increasing more at night. Stratocumulus trends are increasing more during the day in regimes where Sc has positive trends and decreasing more during the day where Sc is declining.

d. Diurnal cycles in base heights of low clouds

The synoptic report includes an estimate of the cloud-base height above the surface. Six-hour average base heights are shown in Fig. 12 for each low cloud type, except fog, which is always based at the surface. Curves are shown for base heights during winter, during summer, and in the tropics. The standard error of the mean for each 6-h period is also shown, indicated by the band surrounding each line. Data for winter and summer are from observations poleward of 30° during each hemisphere's respective winter and summer, so each winter and summer curve represents both hemispheres. Data for the tropics are from observations between 30°N and 30°S during all seasons. The curves are based on 3-h average data over land and 6-h average data over the ocean. Each data point is based on the land- or ocean-area-weighted average of all contributing grid boxes. To better show the shape of each curve, different scales are used for the vertical axes for the different cloud types.

Figure 12 shows that diurnal cycles of base heights are larger over land than over ocean. Tropical and summertime diurnal cycles in base height appear most uniform for all types, with peaks between 1500 and 2100 local time in each frame. The curves suggest that clouds over land reach their peak base height later in the day during summer than during winter. Except for St, summertime extratropical cloud bases are higher than in winter or in the tropics. The afternoon maximum in base height is likely due to the lower relative humidity in the

afternoon, caused by the larger difference between temperature and dewpoint during the warm part of the day (e.g., Betts et al. 2013, their Fig. 3; Sui et al. 1997, their Fig. 8). If the water vapor mixing ratio is held constant and temperature is increased, the level at which a rising air parcel reaches saturation will be higher.

Maritime stratiform clouds (Sc and St) are unique in showing wintertime height maxima during the night, which invites an alternative explanation. It is possible that wintertime fog may be rising from the surface in the morning to a height of a few hundred meters during afternoon, then descending again at night. If this were the case, we would expect to see a later peak for St and Sc amounts in fog regimes, since fog would first be lifted, then reclassified by an observer as St or Sc before thinning, dissipating, or descending later in the day. This is apparent in Fig. 10 where in oceanic fog regimes St and Sc amounts show a delayed diurnal cycle. We also find that the frequency of oceanic St reports during winter is greatest between 1200 and 1800 local time, and not when St amount-when-present peaks between 0600 and 0900 local time. This further suggests that fog is lifting from the surface to a low height, and is then reclassified by observers as stratus cloud, so if we were to group fog together with St as a single type, its diurnal cycle in wintertime base height would likely match that of the other types in "fog" regimes.

4. Discussion

This climatology suggests that the phase of the diurnal cycle is a characteristic of cloud type while the amplitudes vary depending on the local climate. Bergman and Salby (1996) used International Satellite Cloud Climatology Project (ISCCP)-C2 satellite data to diagnose two categories in the diurnal cycles of low clouds, one "maritime non-convective" and the other "continental." They reached a similar conclusion to what we find here, stating that the phase of the diurnal cycle is "uniform within individual categories, which makes cloud diurnal variations independent of geographical location and, therefore, highly spatially coherent."

Kondragunta and Gruber (1996) also used the ISCCP-C2 data to diagnose diurnal cloud properties. They used EOF analysis to identify two modes of the diurnal cycle. Mode 1 of their analysis, identified as the low-cloud diurnal cycle, corresponds to a combination of Bergman and Salby's two low-cloud categories, with maxima in the early morning and midafternoon. Kondragunta and Gruber further showed that the afternoon "continental" maximum is more prevalent inland, in western boundary currents, and during the warmer part of the year. The early morning maximum, Bergman and Salby's maritime

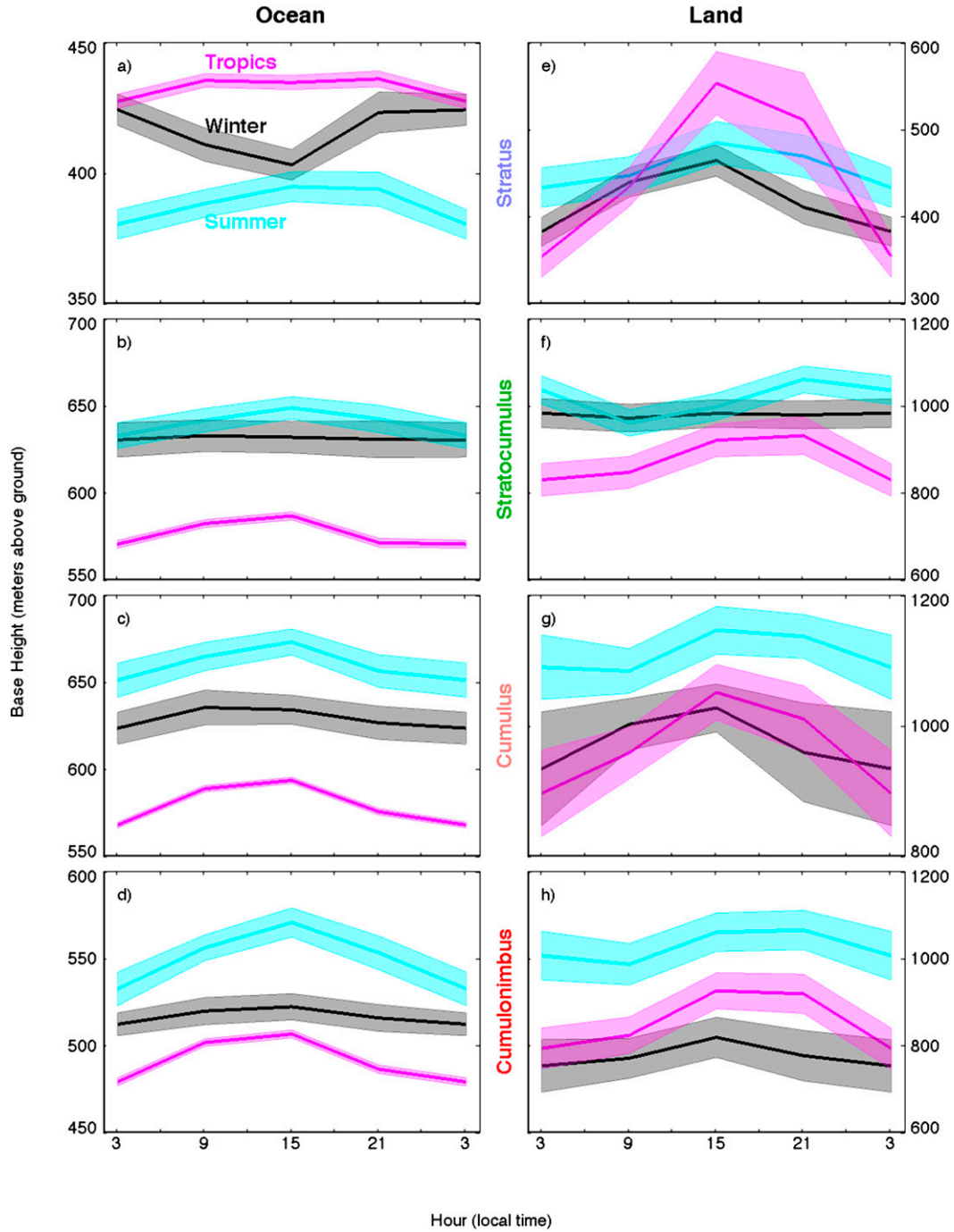


FIG. 12. Average diurnal cycles of low-cloud base heights. Winter and summer data are from areas poleward of 30° during DJF and JJA in each hemisphere’s respective winter and summer seasons. Tropical data are from between 30°N and 30°S during all seasons. Curves shown are land-area-weighted or ocean-area-weighted average base heights calculated over 6-h intervals. Error bars shown are the standard error of the mean for each 6-h interval.

non-convective category, is dominant in those same regions during the cold time of the year. Mode 2 of Kondragunta and Gruber’s analysis corresponds to the diurnal cycle of high cloudiness, and explains 25% of the

normalized variance in total cloud cover, less than half of the 58% explained by mode 1.

Yang et al. (2008) showed that diurnal precipitation maxima are observed near the time of cloud maxima

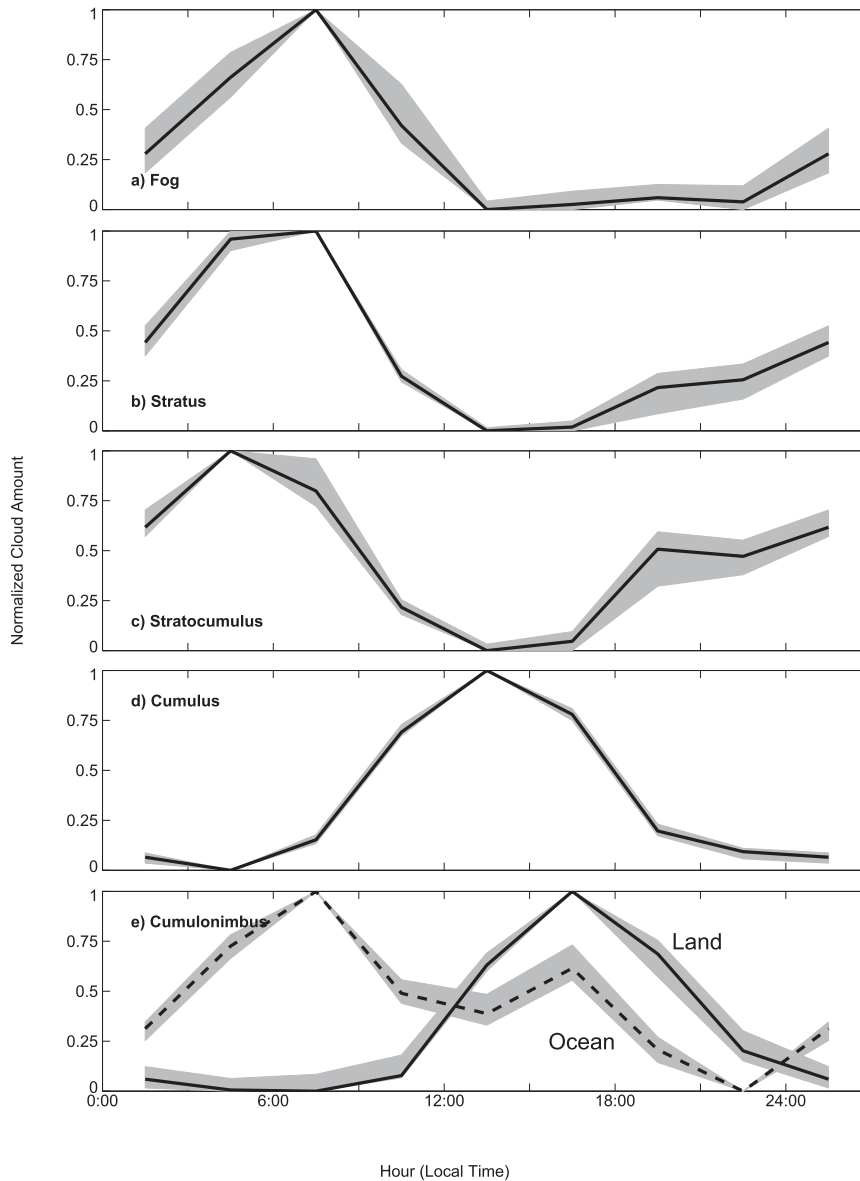


FIG. 13. Diurnal cycles of each cloud type, normalized to a peak value of 1.0 and a minimum of 0.0 over land and ocean areas combined. The thick line is the annual average; the seasonal spread is shown by the gray regions. Cycles were calculated using normalized cycles from each contributing grid box. Area-weighted average cycles were first calculated for land and ocean separately, then the separate land and ocean cycles were averaged, weighted by relative land and ocean area, except in (e). The resulting global averages were then normalized to between 0 and 1 for each season. The seasonal cycles were then averaged to form the annual average, which was again normalized between 0 and 1.

shown in those papers and in this work. Those maxima occur in the late evening/early morning (associated with stratiform drizzle) and the mid to late afternoon (associated with convection from surface heating). The two maxima are not mutually exclusive geographically: individual regions typically show two peaks, with one dominant, and the dominant peak changes with season.

Our analysis using surface observations further corroborates those studies but in addition separates the diurnal cycles by cloud type. Fog, stratus, and stratocumulus agree in their phase to form the combined maritime non-convective mode, peaking in the morning along with maritime cumulonimbus. The phases of cumulus and cumulonimbus (over land) correspond with the continental

mode, with the earlier Cu peak suggesting that Cu frequently builds in to Cb throughout the afternoon. Our work and Yang et al.'s analysis of precipitation data show that these diurnal modes exist together. In any region one cloud type may dominate the cycle, but each individual type is behaving in its own manner together with the rest. To clearly show the proprietary cycle of each cloud type, normalized global mean diurnal cycles are shown in Fig. 13, with land and ocean areas combined except in the case of cumulonimbus. These curves are based on the area-weighted average of the normalized diurnal cycle in every box, then normalized again so that each cycle has minima and maxima of 0 and 1. The seasonal spread and annual average are shown.

Strong positive correlation between day and night trends agrees with the land cloud analysis of Warren et al. (2007). Here we show that the correlation holds for ocean areas as well. We also show that significant trends are either equivalent in magnitude between day and night or greater during the half of the day when clouds are more prevalent. The overall agreement between day and night trends suggests that changes in low cloud cover produce opposing heating and cooling effects during the day versus night. At the surface an increase in cloud cover should result in cooler days and warmer nights, while a decrease would have the opposite effect, except in areas where daytime solar elevation is low. Relationships between season, cloud cover, and surface temperature are shown in more detail in Fig. 16 of Warren et al. (2007).

5. Summary

Based on surface observations we have shown that diurnal cycles are proprietary to each low cloud type. Some latitudinal variation is seen, but in general each cloud type exhibits its own behavior regardless of the climate regime, with the exception of cumulonimbus, which has distinct continental and maritime modes. Fog, stratus, and stratocumulus cloud amounts all peak in the early morning near sunrise, then decrease until the early evening. Stratiform clouds tend to peak later over land than over the ocean. Cumulus cloud amounts peak just after noon. Some cumulus clouds build further into cumulonimbus clouds, peaking in the late afternoon in continental regions and in ocean regions nearer land. However, over the remote ocean cumulonimbus clouds show a maximum in the early morning. Many ocean areas show two diurnal peaks for cumulonimbus.

We find that groups of grid boxes whose diurnal cycle is dominated by the same cloud type form geographically contiguous regions. These regions change with season, especially over land and in the Northern Hemisphere.

Continental regions have diurnal cycles driven by cumuliform clouds during summer and stratiform clouds during winter. Ocean areas and west coasts tend to have diurnal cycles dominated by stratiform clouds year-round. Diurnal cycles over the ocean are only occasionally driven by cumuliform clouds, mostly near the equator or near landmasses.

Multidecadal trends in cloud amounts are small in magnitude and are of the same sign during day and night. These trends can either increase or decrease the diurnal temperature range depending on the sign of the trend. When comparing trends that are 95% significant, some cloud types tend to show larger trends during the half of the day when they are more prevalent, while others show no preference.

The base heights of low clouds typically peak in midafternoon or early evening with two exceptions, both over the ocean during winter. There, cumulonimbus cloud bases are highest in the early morning and stratiform cloud bases are highest at night, the latter possibly due to a bias involving the reporting of fog. Base heights are lower and diurnal cycles are smaller over the ocean than over land. Over land, diurnal cycles of base heights appear to peak later in summer than in winter.

This climatology was produced exclusively from human-made visual cloud observations from weather stations and ships. The data we used are freely available for grid boxes (at <http://cdiac.ornl.gov/ftp/ndp026e/>) and for individual weather stations (at <http://cdiac.ornl.gov/ftp/ndp026d/>). The data can be used for assembling a regional diurnal climatology or verifying a diurnal cloud cycle generated by a model or from other observations.

Acknowledgments. Carole Hahn produced the EECRA for ship observations and began the analysis of diurnal cycles (e.g. Hahn et al. 1995). We acknowledge discussions with her over the past 30 years about analyzing surface cloud observations for diurnal cycles. We thank Mike Pritchard, Mike Wallace, and Robert Wood for helpful discussion. The paper benefitted from comments by two anonymous reviewers. This work was supported by NSF Grant AGS-1021543.

REFERENCES

- Bajuk, L. J., and C. B. Leovy, 1998: Are there real interdecadal variations in marine low clouds? *J. Climate*, **11**, 2910–2921, doi:10.1175/1520-0442(1998)011<2910:ATRIVI>2.0.CO;2.
- Bergman, J. W., and M. L. Salby, 1996: Diurnal variations of cloud cover and their relationship to climatological conditions. *J. Climate*, **9**, 2802–2820, doi:10.1175/1520-0442(1996)009<2802:DVOCCA>2.0.CO;2.

- Betts, A. K., R. Desjardins, and D. Worth, 2013: Cloud radiative forcing of the diurnal cycle climate of the Canadian Prairies. *J. Geophys. Res.*, **118**, 8935–8953, doi:10.1002/jgrd.50593.
- Duynkerke, P. G., 1993: The stability of cloud top with regard to entrainment: Amendment of the theory of cloud-top entrainment instability. *J. Atmos. Sci.*, **50**, 495–502, doi:10.1175/1520-0469(1993)050<0495:TSOCTW>2.0.CO;2.
- Eastman, R., and S. G. Warren, 2013: A 39-yr survey of cloud changes from land stations worldwide 1971–2009: Long-term trends, relation to aerosols, and expansion of the tropical belt. *J. Climate*, **26**, 1286–1303, doi:10.1175/JCLI-D-12-00280.1.
- , —, and C. J. Hahn, 2011: Variations in cloud cover and cloud types over the ocean from surface observations, 1954–2008. *J. Climate*, **24**, 5914–5934, doi:10.1175/2011JCLI3972.1.
- Gray, W. M., and R. W. Jacobson, 1977: Diurnal variation of deep cumulus convection. *Mon. Wea. Rev.*, **105**, 1171–1188, doi:10.1175/1520-0493(1977)105<1171:DVODCC>2.0.CO;2.
- Hahn, C. J., S. G. Warren, and J. London, 1995: The effect of moonlight on observation of cloud cover at night, and application to cloud climatology. *J. Climate*, **8**, 1429–1446, doi:10.1175/1520-0442(1995)008<1429:TEOMOO>2.0.CO;2.
- , —, and R. Eastman, 2003: Cloud climatology for land stations worldwide, 1971–1996 (updated to 2009 for seasonal averages of individual years). Tech. Rep. NDP-026D, Carbon Dioxide Information Analysis Center, 35 pp. [Available online at <http://cdiac.ornl.gov/ftp/ndp026d/>.]
- , —, and —, 2007: A gridded climatology of clouds over land (1971–96) and ocean (1954–97) from surface observations worldwide (updated to 2008 for seasonal averages of individual years over the ocean). Carbon Dioxide Information Analysis Center Rep. NDP-026E, 71 pp. [Available online at <http://cdiac.ornl.gov/ftp/ndp026e/>.]
- , —, and —, 2009: Extended edited synoptic cloud reports from ships and land stations over the globe, 1952–1996 (updated to 2009). Numerical Data Package NDP-026C, Carbon Dioxide Information Analysis Center (CDIAC). [Available online at <http://cdiac.ornl.gov/epubs/ndp/ndp026c/ndp026c.html>.]
- Hignett, P., 1991: Observations of diurnal variations in a cloud-capped marine boundary layer. *J. Atmos. Sci.*, **48**, 1474–1482, doi:10.1175/1520-0469(1991)048<1474:OODVIA>2.0.CO;2.
- Kondragunta, C. R., and A. Gruber, 1996: Seasonal and annual variability of the diurnal cycle of clouds. *J. Geophys. Res.*, **101**, 21 377–21 390, doi:10.1029/96JD01544.
- Loeb, N. G., B. A. Wielicki, D. R. Doelling, G. L. Smith, D. F. Keyes, S. Kato, N. Manalo-Smith, and T. Wong, 2009: Toward optimal closure of the Earth's top-of-atmosphere radiation budget. *J. Climate*, **22**, 748–766, doi:10.1175/2008JCLI2637.1.
- Norris, J. R., 1999: On trends and possible artifacts in global ocean cloud cover between 1952 and 1995. *J. Climate*, **12**, 1864–1870, doi:10.1175/1520-0442(1999)012<1864:OTAPAI>2.0.CO;2.
- Rozendaal, M. A., C. B. Leovy, and S. A. Klein, 1995: An observational study of the diurnal cycle of marine stratiform cloud. *J. Climate*, **8**, 1795–1809, doi:10.1175/1520-0442(1995)008<1795:AOSODV>2.0.CO;2.
- Smith, A., N. Lott, and R. Vose, 2011: The integrated surface database: Recent developments and partnerships. *Bull. Amer. Meteor. Soc.*, **92**, 704–708, doi:10.1175/2011BAMS3015.1.
- Stubenrauch, C. J., A. Chédin, G. Rädcl, N. A. Scott, and S. Serraz, 2006: Cloud properties and their seasonal and diurnal variability from TOVS Path-B. *J. Climate*, **19**, 5531–5553, doi:10.1175/JCLI3929.1.
- Sui, C.-H., K.-M. Lau, Y. N. Takayabu, and D. A. Short, 1997: Diurnal variations in tropical ocean cumulus convection during TOGA COARE. *J. Atmos. Sci.*, **54**, 639–655, doi:10.1175/1520-0469(1997)054<0639:DVITOC>2.0.CO;2.
- Warren, S. G., R. Eastman, and C. J. Hahn, 2007: A survey of changes in cloud cover and cloud types over land from surface observations, 1971–1996. *J. Climate*, **20**, 717–738, doi:10.1175/JCLI4031.1.
- Weare, B. C., 1999: Combined satellite and surface-based observations of clouds. *J. Climate*, **12**, 897–913, doi:10.1175/1520-0442(1999)012<0897:CSASBO>2.0.CO;2.
- WMO, 1956: *International Cloud Atlas*. World Meteorological Organization, 72 plates, 62 pp.
- , 1974: Manual on codes. Vol. 1. World Meteorological Organization Publication 306, 348 pp.
- Wood, R., 2012: Stratocumulus clouds. *Mon. Wea. Rev.*, **140**, 2373–2423, doi:10.1175/MWR-D-11-00121.1.
- Woodruff, S. D., R. J. Slutz, R. L. Jenne, and P. M. Steurer, 1987: A comprehensive ocean–atmosphere data set. *Bull. Amer. Meteor. Soc.*, **68**, 1239–1250, doi:10.1175/1520-0477(1987)068<1239:ACOADS>2.0.CO;2.
- , H. F. Diaz, J. D. Elms, and S. J. Worley, 1998: COADS release 2 data and metadata enhancements for improvements of marine surface flux fields. *Phys. Chem. Earth*, **23**, 517–526, doi:10.1016/S0079-1946(98)00064-0.
- Worley, S. J., S. D. Woodruff, R. W. Reynolds, S. J. Lubker, and N. Lott, 2005: ICOADS release 2.1 data and products. *Int. J. Climatol.*, **25**, 823–842, doi:10.1002/joc.1166.
- Wylie, D., 2008: Diurnal cycles of clouds and how they affect polar-orbiting satellite data. *J. Climate*, **21**, 3989–3996, doi:10.1175/2007JCLI2027.1.
- Yang, S., K.-S. Kuo, and E. A. Smith, 2008: Persistent nature of secondary diurnal modes of precipitation over oceanic and continental regimes. *J. Climate*, **21**, 4115–4131, doi:10.1175/2008JCLI2140.1.